

Grain shape effect on dielectric properties and ionic conductivity of Gd-doped ceria

S. A. Acharya*, K. Singh

Department of Physics, rashtrasant Tukdoji Maharaj Nagpur University, Nagpur 440033, M.S. India

*Corresponding author. E-mail: saha275@yahoo.com

Received: 06 January 2013, Revised: 25 March 2013 and Accepted: 01 May 2013

ABSTRACT

Dielectric behaviour and ionic conductivity of nanostructured $\text{Ce}_{0.9}\text{Gd}_{0.1}\text{O}_{2-\delta}$ (GDC) are investigated to probe morphology influence of grains on ion transport mechanism at microscopic level. GDC are synthesized in two different morphologies of grains (rod-shape and round-shape particles). TEM study confirmed shape and size; diameter of rods are observed around 20 nm and length are in range of 50-100 nm, while diameter of round particles are found about 10 nm. The dielectric behaviour is studied using the dielectric functions such as dielectric permittivity (ϵ') and electric modulus (M''). The ionic conductivity is studied by temperature dependent impedance spectra. Both these properties are observed to be finely manipulative by morphology and size. Activation energy of charge carrier relaxation and charge carrier orientation are calculated from impedance spectra and electric modulus spectra and are found to be more in rod-shape GDC. Dielectric relaxation times are also observed to be more for GDC rods. This study provides clear evidence that grain shape and size affect on dopant-oxygen vacancies interaction, which affect on ion migration and hence ionic conductivity. 1D morphology of grains in oxy-ion conductor has high potential to enhance ionic conductivity. Copyright © 2014 VBRI press.

Keywords: Gd-doped ceria; rods-shape and round-shape morphology; ionic transport mechanism; dielectric relaxation.



Smita A. Acharya did Ph.D. at R.T.M. Nagpur University. She completed her postdoctoral work at Pune University. Her main research activities includes synthesis of ceramics in different morphology at nanoscale and studies their impact on physical properties. Her current research are focused on synthesis of semiconductor nanostructure, solid electrolyte for SOFC, Fe and Mn based perovskite multiferroic by soft chemical route for different applications view point. She has more than 25 research paper in various reputed international journals.



Kamal Singh, retired Professor and Head, dept. of physics, RTM Nagpur university. She was V.C. of SGB Amaravati University. Her major work embodies Solid State Ionics and Ferroelectrics. Solid State Ionic materials include solid electrolytes and mixed conductors, and are building stones for several solid state ionic devices such as solid state batteries, sensors, fuel cells, electrochromic display, high temperature electrolyzers, gas separation membranes, etc. Before this, acquired considerable experience in the field of ferroelectrics, ceramics, glasses, glass-ceramics etc. during the Ph. D and, particularly, Post Doc. fellowship at Metallurgical Department of IIT Kanpur. She has published more than 200 research paper and filed 6 patents. She supervised 30 research students for Ph.D degree.

Introduction

Ceria-based solid electrolytes have been attracting great interest for applications in oxygen sensors [1-2], solid oxide fuel cells [3-5], oxygen pumps and oxygen permeable membrane catalysts, due to high oxygen ionic conductivity [6-9]. Amongst these, solid oxide fuel cell (SOFC) is extensively attended and demonstrated as a clean and efficient power source for generating electricity from variety of fuels [10-15]. SOFC operating temperature and efficiency is decided by oxy-ion conducting ability of electrolytes. So, electrolytes having fast migration of oxygen ions are highly desirable.

Searching out of new oxy-ion conductors or optimization of the existing electrolytes materials for enhancement of ionic conductivity is the current R & D focus for intermediate temperature SOFC development. To optimize the existing electrolytes, influences of microstructure feature on ionic conductivity are needed to be investigated at atomic scale. Nanocrystalline materials have been expected to improve electrochemical properties and perform better than microcrystalline ones [16-22]. It is commonly observed that in nanostructure materials, electrical conductivity is significantly influenced by grain size, homogeneity in grain size and grain shape [23-26]. But, the detail effects of the nanoscale on ionic conductivity in particular and ionic transport mechanism in general are still relatively unknown. It is very important to study oxy-ion diffusion phenomenon at microscopic level for

fundamental understanding of ion transport in nanostructure doped ceria system. The size-morphology influence of grain on ion transport mechanism can be predicted from ion relaxation process on grain (G) and grain boundaries (GB). The dynamics of electrical process have been well understood at atomic level by correlating dielectric behaviour with ionic conducting phenomenon for different dielectrics systems such as perovskite multiferroics, ferroelectrics, antiferroelectrics etc [27-31]. It creates curiosity to investigate the role of size and morphology of grains on charge relaxation and transport phenomenon of fluorite-structured ceramics system (rare-earth doped-ceria). In present work, correlation of dielectric properties and ionic conductivity are investigated for the nanostructured $\text{Ce}_{0.9}\text{Gd}_{0.1}\text{O}_{2-\delta}$ (GDC) in two different morphologies of grains (rod-shape and round-shape particles). The dielectric behaviour is studied using the dielectric functions such as dielectric permittivity (ϵ') and electric modulus (M''). The charge relaxation processes of rod-shape and round grain and respective grain boundaries were systematically investigated. The ionic transport mechanism was probed by temperature dependent ionic conductivity and impedance spectra. As per our knowledge, it is the first attempt to study charge relaxation process in rod-shape grains in Gd-doped ceria.

Experimental

For synthesis of Gadolinium-doped-ceria (GDC), raw chemicals were used as follows: cerium nitrate hexahydrate and gadolinium (III) nitrate hexahydrate (99.9% purity, procured from Sigma Aldrich, Germany). These chemicals were prepared as 0.5 M solutions using double distilled water. The gadolinium nitrate hexahydrate solution was mixed with the cerium nitrate hexahydrate solution according to the molar ratio 1:9 with vigorous magnetic stirring. An appropriate amount of sodium carbonate (Merck) was added in order to co-precipitate the cations. In order to control the particle morphology, the pH value was varied from 8 to 14. For each pH value, the reaction was proceed at room temperature with vigorous magnetic stirring for 1 hr. The precipitate was separated by centrifugation and dried in an oven at 80°C for overnight. The precursor was calcined at 700°C for 2 h to obtain single phase nanocrystalline materials.

Sample characterization

The morphology of the samples was observed using a scanning electron microscope (SEM, JEOL-6360) and transmission electron microscope (TEM, Technai 20G²) operated at an accelerating voltage of 200 keV using carbon coated formvar grids. The sample was prepared by dispersing the nanostructures in N, N-dimethylformamide (DMF) using ultrasonication. The average grain size was calculated using the linear intercept method measuring more than 200 grains from SEM. The crystal phases of the specimens were identified using a X-ray diffraction (XRD) using a Bruker D8 Advance X-ray diffractometer with $\text{CuK}\alpha$ radiation at a scanning rate of 1 min^{-1} . The calcined powders were well milled in an agate mortar. The powder was pressed uniaxially under 250 MPa to form green

pellets of a 9 mm diameter and an approximately 1 mm thickness. The pressed pellets were sintered by microwave and by the conventional mode of heating. The microwave sintering assembly was designated in-house and was fabricated by modifying a domestic microwave oven. For conventional sintering, a locally made, high temperature muffle furnace was used. The sintering conditions were optimized for temperature and time for both heating methods.

The best sintering results were obtained by microwave at 950 °C for 1 h and by conventional furnace at 1400 °C for 4 h with a heating rate of 5 °C min^{-1} . The relative density was calculated as the ratio of the mass of the atoms in the unit cell to the volume of the unit cell by the lattice parameter, and the sintered density was determined using the Archimedes method. The rod-shape morphology was found to be modified into roughly round grains by conventionally sintered pellet, while microwave proceed dense pellets were observed to be sustained morphology and control grain-growth during sintering. Hence microwave-assisted sintered pellets were used for electrical characterization of the samples.

The ionic transference number (t_{ion}) and the electronic transference number (t_{ele}) in the nanostructured Gd-doped ceria at 450 °C in air were calculated using the Wagner's polarization technique. The dielectric constant ϵ' , electric modulus M'' and AC impedance measurements were carried out in air in the temperature range of 300-600 °C and the frequency range of 5 Hz to 13 MHz by conventional two probe method using HP-4191A Impedance analyzer. Silver paste was used on both sides of the pellet with diameter for the purpose of electrodes. The density of the pellets sintered by microwave and conventional route was about 95% of the theoretical density. These pellets used in both DC polarization technique and impedance measurement.

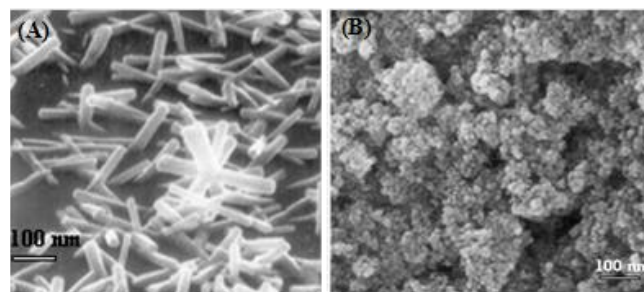


Fig. 1. SEM images of GDC (A) rod-shape (B) round-shape nanoparticles.

Result and discussion

The SEM images of calcined GDC samples prepared by varying P_{H} of reaction are shown in Fig. 1. The rod-shape particles were obtained when the P_{H} was maintained to 9 by sodium carbonate solution and the round shape particles were obtained for P_{H} was adjusted to 14.

In Fig. 2, TEM images of the primary particles of the nanosized particles of both morphologies types are presented. The average particles sizes of the round shaped and rod-shape particles were approximately 10 and 20 nm, respectively.

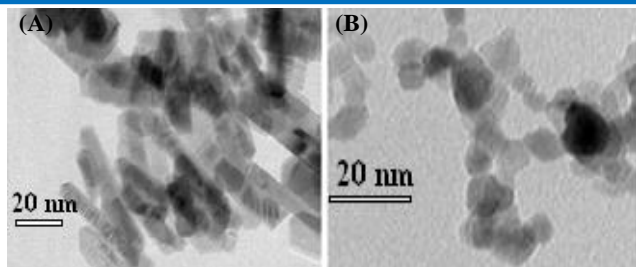


Fig. 2. TEM images of GDC (A) rod-shape (B) round-shape nanoparticles.

XRD profiles of the differently shaped GDC particles are shown in Fig. 3. Both profiles are identical and indicated the presence of a single phase cubic fluorite related structure (when compared with JCPDS data base). Broad nature of XRD peaks are clear evidence for fine nature of our product.

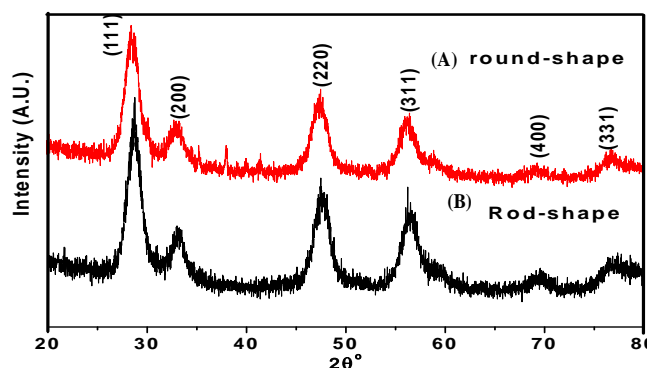


Fig. 3. XRD profiles of GDC (A) round shape particles (B) rod-shape particles.

In the dc polarization technique, the pellets were polarized by supplying a dc voltage of 250 mV for about 6 h and the current values were monitored by Keithley source meter. The Wagner polarization techniques employ asymmetric electrode configuration with one blocking and the other reversible electrode in the opposite side. In this configuration, blocking electrode can be blocking either ionic or electronic current. So we get pure electronic or pure ionic information of our samples. In the present work to know the effect of morphology on the ionic transference number of the rods-shape and round-shape particles of GDC samples, the current versus time graph by polarizing the cell with DC voltage 250 mV by following the Wagner's polarization techniques are studied (Fig. 4).

The ionic and electronic transference numbers (t_{ion} and t_{ele} , respectively) are calculated using the following equations:

$$t_{ion} = (I_i - I_f) / I_i \quad (1)$$

where, I_i is the initial current and I_f is the final current.

The value of ionic transference number is found to be 0.87 for rod-shape and 0.81 for round-shape particles at 500 °C in air. The ionic transference number for rods-shape particles are more than the round-shape particles.

It suggests that charge transport in these nanocrystalline materials is due to ions and more ionic charge availability. The variation of ionic transport number is purely due to morphology effect.

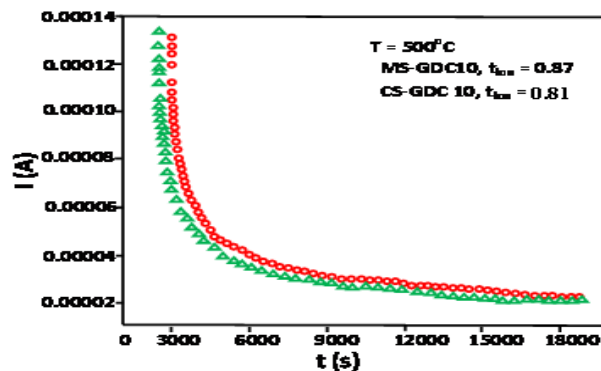


Fig. 4. The current versus time plot of the MS-GDC10 and CS-GDC10.

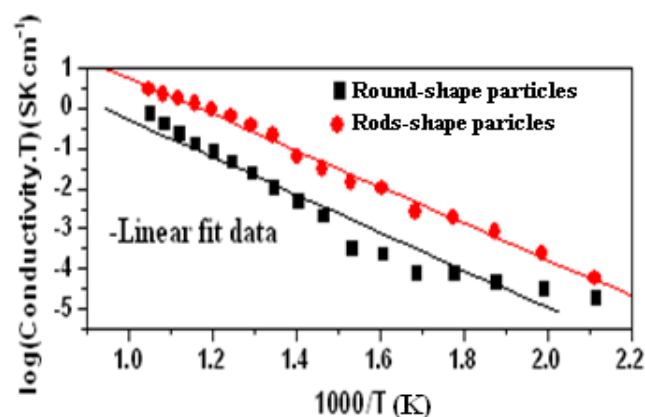


Fig. 5. Arrhenius plots ionic conductivities of GDC samples in different morphology.

Fig. 5 shows the Arrhenius plot of $\log(\sigma T)$ vs $1000/T$ (K), where σ is total conductivity. The conductivity of these nanocrystalline materials at 500°C is found to be $1.54 \times 10^{-2} \text{ Scm}^{-1}$ and $3.78 \times 10^{-3} \text{ Scm}^{-1}$ with activation energy (E_a) of 0.99 eV and 1.06 eV for rod-shape and round-shape GDC particles. In case of rod-shape particles all the data points fall in a single straight line and follow the Arrhenius behaviour, while for round-shape particles, conductivity slightly deviates from the Arrhenius behaviour. The deviation in the Arrhenius behaviour can be speculated as inhomogeneity in the grain. Dopant-oxygen vacancy interaction is one of the reasons for inhomogeneity.

The variations of imaginary part of impedance (Z'') with frequency at different temperature are shown in Fig. 6 (A & B). Each plot contains a relaxation peak at higher frequency corresponding to bulk conduction. The peaks are found to be shifted towards higher frequency side with increasing temperature. Same trends are observed for both the samples.

The curves are asymmetric and broader than the ideal Debye peak. The relaxation time is obtained from the reciprocal of the peak frequency which shifts to lower values with increase in temperature and it is found to obey the Arrhenius relation as shown in the inset to the Fig 6A.

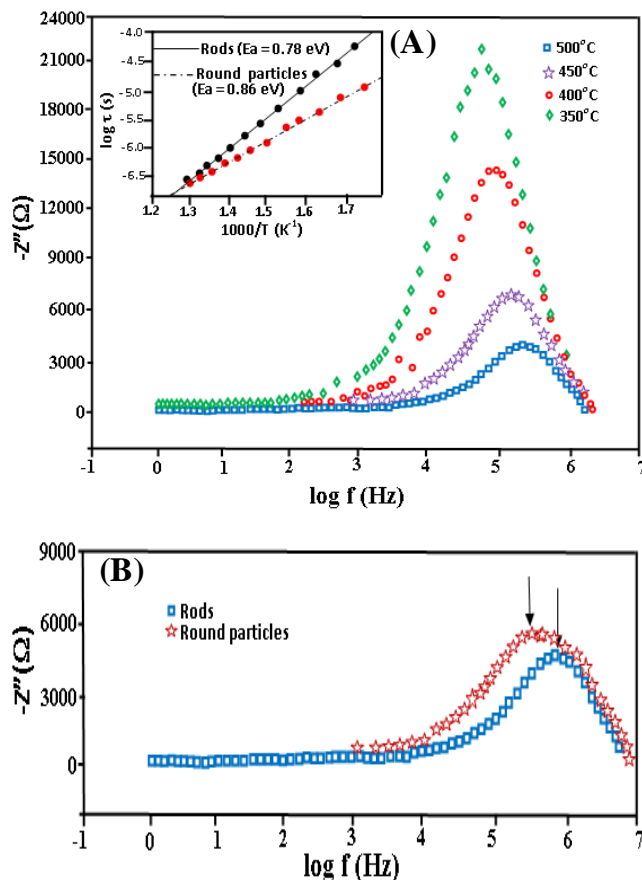


Fig. 6. Impedance spectra (A) of GDC rods at different temperature. The inset is the Arrhenius plot of relaxation times corresponding to relaxation peaks at various temperatures (B) comparative spectra of rods and round particles at 500 °C.

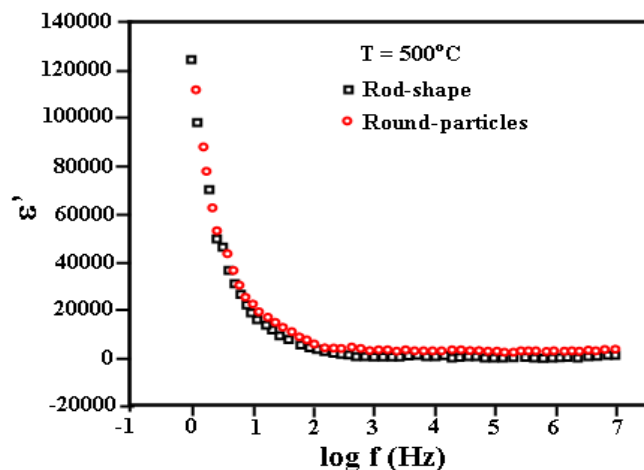


Fig. 7. The variation of real part of permittivity (ϵ') with frequency at 500 °C.

The activation energy corresponding to this non Debye type of relaxation is found to be 0.78 and 0.86 eV for rod-shape and round-shape particles, respectively. Both the values are found to be less than the value of activation energy (E_{σ}) calculated from temperature dependent conductivity. It suggests that the relaxation of charge carriers is associated with migration of charge carrier; have to overcome less energy barriers while relaxing than

conducting. Comparative impedance spectra GDC (**Fig. 6b**) at 500°C clearly show that charge carrier relaxation in rod-shape grains have occurred at slightly more frequency than round particles. Inhomogeneity in grains may create disturbances for charge relaxation. It attributes to more charge carrier relaxation time for round-shape grains than rods of GDC.

Dielectric relaxation of the samples were studied by the variation of real part of permittivity (ϵ') with frequency (as shown in **Fig. 7**). ϵ' with frequency shows a sharp upturn and high values of ϵ' at lower frequencies irrespective of the temperature of measurement. The upturn in ϵ' at lower frequencies is attributed to the polarization of charge carriers at the electrode-electrolyte interface. The decrease in ϵ' with increase in frequency is due to high periodical reversal of field at the interface, which reduces the contribution of charge carriers to the dielectric constant and finally it saturates at higher frequencies giving rise to dielectric constant ϵ_{∞} . The values of dielectric constant ϵ_{∞} for rod-shape particles are found to be around 5.3 and 12.17 at 400 and 500°C, respectively. However, the values of ϵ_{∞} for round shape particles are obtained to be about 3.5 and 10.24 at 400 and 500 °C, respectively. Also the dielectric relaxation ratios ($r = \epsilon_s / \epsilon_{\infty}$, where ϵ_s is zero frequency limit of ϵ') for rod-shape particles are found to be 4703.4 and 12145.9, respectively, at 400 and 500°C. While for round shape particles, it is obtained to be 3918.6 and 10125.3, respectively, at 400 and 500°C. For both the values are high. The high value of dielectric relaxation ratio suggests that there exist a long range order migration of oxygen ions. The comparative high value of dielectric relaxation time of rod-shape than round-shape nanoparticles of GDC, clearly indicate that the range of order migration of oxygen ions is more in rod-shape than round-shape particles in the temperature range 300 – 500°C.

In order to suppress the polarization effect at lower frequencies and for studying conduction process in more detail, the data are converted into electric modulus. The variations of imaginary part of electric modulus M'' with frequency at various temperatures are shown in **Fig. 8**.

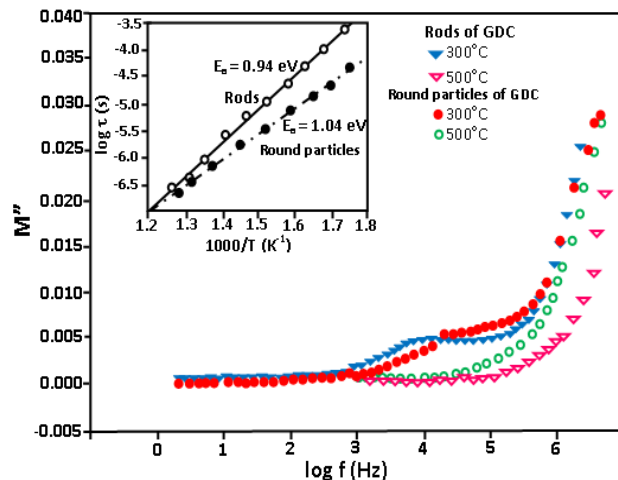


Fig. 8. Variation of imaginary part of electric modulus (M'') with frequency at different temperature. the inset is the Arrhenius plot of relaxation time corresponding to reorientation process.

At lower frequencies, the values of M'' approach to zero and it indicates that the electrode polarization does not make any significant contribution to the modulus data. At lower temperatures the modulus spectra contain single relaxation peak and the curve moves towards M_∞ at higher frequency. The peak attributes to the charge reorientation relaxation of defect associates $(Gd^{3+}-V_o)^*$ present in this materials, as observed by Sarkar and Nicholson [32]. With increase in temperature, the relaxation peak is found to shift towards the higher frequency with slow decrease in the peak height and finally at very high temperature M'' tends to M_∞ . This suggests that a thermally activated process is responsible and at elevated temperatures there exist a mobility of charge carriers from short range to long range [33]. The decrease in peak height corresponds to the dissociation of bound pairs because of high mobility of oxygen vacancy at elevated temperatures. The activation energy for reorientation of oxygen vacancy is calculated from Arrhenius plot (shown as inset in Fig. 8. of relaxation times which are the reciprocal of peak frequencies (f_M'')) and it is found to be 0.94 eV for rod-shape particles and 1.04 eV for round-shape particles. The motion of the V_o^{**} in this reorientation process is bound motion i.e. the oxygen vacancy V_o^{**} remains bound to the Gd^{+3} ion and jumps between the nearest neighbour position of the Gd^{+3} in the cubic system. This jump is similar to that of a free V_o^{**} in the system. The size and morphology of grains influences on the dopant-oxygen vacancy interaction. Thus the energy required for reorientation of V_o^{**} varies with morphology of grains. The variation of activation energy of reorientation of oxygen vacancy in rod-shape particles is more than round-shape particles.

The activation energy of charge carrier relaxation and orientation in rods-shapes are found to be less than round-shape grains. Both the phenomenons are observed to be thermally activated. In ionic conductor charge carrier relaxation and orientation contributes for ion migration. This is responsible for improvement of ionic conductivity in rod-shape compare to round particles of GDC.

Conclusion

The cubic fluorite nanostructures $Ce_{0.90}Gd_{0.10}O_{2-8}$ material having rod-shape and round-shape particles with size 20 and 10 nm, respectively were prepared successfully at room temperature by co-precipitation method. Morphology was found to be changed with varying pH of the reaction. The obtained materials in both the morphologies were ionic in nature at lower temperature range with ionic transference number 0.87 and 0.81 in air at 500°C for rod-shape and round-shape nanoparticles, respectively. Deviation in Arrhenius behaviour for ionic conductivity correlated with inhomogeneity in the grain is due to dopant-oxygen vacancy interaction. The interaction directly affect on activation energy of charge carrier relaxation and reorientation. Hence, rod-shape particles of GDC have less activation energy of charge relaxation and reorientation compared to round-shape particles of GDC, thus increase in comparative ionic conductivity. The 1-D, morphology of grains in oxy-ion conducting ceramics has high future prospective to enhance oxy-ion conductivity.

Acknowledgements

The author acknowledges financial support from DST, New Delhi, India under Fast Track project SR/FTP/PS-106/2009 (G) and UGC under MRP F.N. 41-871/2012.

References

- Fergus J. W., *Sens. Actuators B Chem*, 2007, 121, 652.
DOI: [10.1016/j.snb.2006.04.077](https://doi.org/10.1016/j.snb.2006.04.077).
- Izu N., Shin W, Matsubara I., Murayama N., *Sens. Actuators B Chem*, 2004, 101, 381,
DOI: [10.1016/j.snb.2004.04.011](https://doi.org/10.1016/j.snb.2004.04.011).
- Arico A.S., Sin A., Kopnin E., Dubitsky Y, Zaopo A, La Rosa D., Gullo L.R. Antonucci V., *J Power sources*, 2007, 164, 300.
DOI: [10.1016/j.jpowsour.2006.10.078](https://doi.org/10.1016/j.jpowsour.2006.10.078).
- Riess I., *Solid State Ionics*, 2005, 176 (19-22), 1667.
DOI: [10.1016/j.ssi.2005.04.015](https://doi.org/10.1016/j.ssi.2005.04.015).
- Hamakawa S, Hayakawa T., York A.P.E, Tsunoda T., Yoon Y. S., Suzuki K., Shimizu M., Takehira K, *J Electrochem Soc.*, 1996, 143 (4), 1264.
DOI: [10.1149/1.1836627](https://doi.org/10.1149/1.1836627)
- Luo J., Ball R.J. and Stevens R., *J. Mat. Sci.*, 2004, 39, 235.
DOI: [10.1023/B:JMSE.000007749.72739.bb](https://doi.org/10.1023/B:JMSE.000007749.72739.bb)
- Weppner W., *Solid State Ionics*, 1992, 52, 15.
DOI: [10.1016/0167-2738\(92\)90087-6](https://doi.org/10.1016/0167-2738(92)90087-6)
- Kendall K.R., Navas C., Thomas J.K. and Zur Loye H.C., *Solid state Ionics*, 1995, 82, 215.
DOI: [10.1016/0167-2738\(95\)00207-4](https://doi.org/10.1016/0167-2738(95)00207-4).
- Lane J.A., Benson S.J., Waller D., Kilner J.A., *Solid State Ionics*, 1999, 121, 201.
DOI: [10.1016/S0167-2738\(99\)00014-4](https://doi.org/10.1016/S0167-2738(99)00014-4).
- Patil B B, Pawar S.H., *Appl. Surf.Sci.* 2007, 253 (11), 4994.
DOI: [10.1016/j.apsusc.2006.11.007](https://doi.org/10.1016/j.apsusc.2006.11.007).
- Inaba H., Tagawa H., *Solid State Ionics*, 1996, 83,1.
DOI: [10.1016/0167-2738\(95\)00229-4](https://doi.org/10.1016/0167-2738(95)00229-4)
- Steel B.C.H., *Nature*, 2001, 414 (15), 345.
DOI: [10.1038/35104620](https://doi.org/10.1038/35104620).
- Muecke U.P., Beckel D., Bernard A., Bieberle-Hütter A., Graf S., Infortuna A., Müller P., Rupp J.L.M., Schneider J., Gauckler L.J., *Adv. Funct. Mater.* 2008, 18, 3158.
DOI: [10.1002/adfm.200700505](https://doi.org/10.1002/adfm.200700505).
- Huang H., Nakamura M., Su P., Fasching R., Saito Y., Prinz F.B., *J. Electrochem. Soc.* 2007, 154, B20.
DOI: [10.1149/1.2372592](https://doi.org/10.1149/1.2372592)
- Takagi Y., Lai B.-K., Kerman K., Ramanathan S., *Energy Environ. Sci.* 2011, 4, 3473.
DOI: [10.1039/C1EE01310F](https://doi.org/10.1039/C1EE01310F)
- Bellino M.G., Lamas D.G., DeReca N.E.W., *Adv. Funct. Mater.* 2006, 16,107.
DOI: [10.1002/adfm.200500186](https://doi.org/10.1002/adfm.200500186).
- Jansinski P., *Solid State Ionics*, 2006, 177, 2509.
DOI: [10.1016/j.ssi.2006.04.018](https://doi.org/10.1016/j.ssi.2006.04.018).
- Ruiz-Trejo E., Kilner J.A., *J. appl. Electrochem.* 2009, 39, 523.
DOI: [10.1007/s10800-008-9713-1](https://doi.org/10.1007/s10800-008-9713-1).
- Mondal P, Klein A, Jaegermann W, Hahn H. *Solid State Ion*, 1999,118,3319.
DOI: [10.1016/S0167-2738\(98\)00452-4](https://doi.org/10.1016/S0167-2738(98)00452-4).
- Suzuki T, Kosacki I, Anderson HU, Colombari P, *J Am Ceram Soc*, 2001, 84, 2007.
DOI: [10.1111/j.1151-2916.2001.tb00950.x](https://doi.org/10.1111/j.1151-2916.2001.tb00950.x)
- Kosacki I, Anderson HU, Mizutani Y, Ukai K. *Solid State Ion*, 2002,152-153, 431.
DOI: [10.1016/S0167-2738\(02\)00382-X](https://doi.org/10.1016/S0167-2738(02)00382-X).
- Zhang Y.W., Jin S., Yang Y., Li G.B., Tian S.J., Jia J.T., *Appl Phys Lett*, 2000, 77, 3409.
DOI: [10.1063/1.1328099](https://doi.org/10.1063/1.1328099)
- Fu Y., Wei Z.D., Ji M.B., Li L. and Shen P.K., *J. Zhang, Nanoscale Res. Lett.*, 2008, 3, 431.
DOI: [10.1007/s11671-008-9177-6](https://doi.org/10.1007/s11671-008-9177-6)
- Zhou K., Yang Z., Yang S., *Chem. Mater.*, 2007, 19, 1215.
DOI: [10.1021/cm062886x](https://doi.org/10.1021/cm062886x).
- Sun C., Li H., Wang Z.X., Chen L., and Huang X., *Chem. Lett.*, 2004, 33, 662.
DOI: [10.1246/cl.2004.662](https://doi.org/10.1246/cl.2004.662).
- Zhou K., Yang Z., Yang S., *Chem. Mater.*, 2007, 19, 1215.
DOI: [10.1021/cm062886x](https://doi.org/10.1021/cm062886x).

27. Behera A., Mohanty N. K., Behera B., Nayak P., *Adv. Mat. Lett.* 2013, 4(2), 141.
DOI: [10.5185/amlett.2012.6359](https://doi.org/10.5185/amlett.2012.6359).
28. Barik, S.K.; Choudhary, R.N.P.; Singh, A.K. *Adv. Mat. Lett.* 2011, 2(6), 419.
DOI: [10.5185/amlett.2011.2228](https://doi.org/10.5185/amlett.2011.2228)
29. Sahoo, S.; Pradhan, D.K.; Choudhary, R. N. P.; Mathur, B. K. *Adv. Mat. Lett.* 2012, 3(2), 97.
DOI: [10.5185/amlett.2011.4250](https://doi.org/10.5185/amlett.2011.4250).
30. Rosaiah P., Hussain O. M., *Adv. Mat. Lett.* 2013, 4(4), 288
DOI: [10.5185/amlett.2012.8416](https://doi.org/10.5185/amlett.2012.8416).
31. Parida, B. N.; Das, P.R.; Padhee, R.; Choudhary, R. N. P. *Adv. Mat. Lett.* 2012, 3(3), 231
DOI: [10.5185/amlett.2012.2321](https://doi.org/10.5185/amlett.2012.2321)
32. Sarkar P. and Nicholson P.S., *J. Amer. Ceram. Soc.*, 1989, 72, 1447.
DOI: [10.1111/j.1151-2916.1989.tb07672.x](https://doi.org/10.1111/j.1151-2916.1989.tb07672.x)
33. Kumar A. and Manna I., 2008, *Physica B*, 403, 2298.
DOI: [10.1016/j.physb.2007.12.009](https://doi.org/10.1016/j.physb.2007.12.009).

Advanced Materials Letters

Publish your article in this journal

[ADVANCED MATERIALS Letters](#) is an international journal published quarterly. The journal is intended to provide top-quality peer-reviewed research papers in the fascinating field of materials science particularly in the area of structure, synthesis and processing, characterization, advanced-state properties, and applications of materials. All articles are indexed on various databases including [DOAJ](#) and are available for download for free. The manuscript management system is completely electronic and has fast and fair peer-review process. The journal includes review articles, research articles, notes, letter to editor and short communications.

